Organic & Biomolecular Chemistry

PAPER

View Article Online
View Journal | View Issue

Cite this: *Org. Biomol. Chem.*, 2015, **13**, 8453

A quantum chemical study of the ω-transaminase reaction mechanism†

Karim Engelmark Cassimjee, Bianca Manta and Fahmi Himo*

Received 7th April 2015,
Accepted 30th June 2015

DOI: 10.1039/c5ob00690b

www.rsc.org/obc

ω-Transaminases are valuable tools in biocatalysis due to their stereospecificity and their broad substrate range. In the present study, the reaction mechanism of *Chromobacterium violaceum* ω-transaminase is investigated by means of density functional theory calculations. A large active site model is designed based on the recent X-ray crystal structure. The detailed energy profile for the half-transamination of (*S*)-1-phenylethylamine to acetophenone is calculated and the involved transition states and intermediates are characterized. The model suggests that the amino substrate forms an external aldimine with the coenzyme pyridoxal-5′-phosphate (PLP), through geminal diamine intermediates. The external aldimine is then deprotonated in the rate-determining step, forming a planar quinonoid intermediate. A ketimine is then formed, after which a hemiaminal is produced by the addition of water. Subsequently, the ketone product is obtained together with pyridoxamine-5′-phosphate (PMP). In the studied half-transamination reaction the ketone product is kinetically favored. The mechanism presented here will be valuable to enhance rational and semi-rational design of engineered enzyme variants in the development of ω-transaminase chemistry.

I. Introduction

Transaminases, or aminotransferases, are enzymes capable of catalyzing the interchange of amino and keto groups by utilizing the coenzyme pyridoxal-5′-phosphate (PLP).[1] In the cellular metabolism, biosynthesis of amino acids can be performed by transamination of the corresponding keto acids.[2] Transaminases are usually classified based on their substrate scope. ω-Transaminases (ωTAs) accept substrates that can have several carbons between the carboxylate and the amino group. An interesting feature of ωTAs is that they may accept ketones and amines without carboxyl groups as substrates, generally with high enantiospecificity and a relatively broad substrate range.[3,4] These properties are useful in chemical applications where synthesis of chiral amines from prochiral precursors is desired, *e.g.* in pharmaceutical production. It has been shown that ωTAs can be used as catalysts in kinetic resolution and stereoselective synthesis of optically pure amines.[5] Employment on a large scale for pharmaceutical synthesis has also been demonstrated.[6]

A broad range of enzymes utilize PLP as a coenzyme.[7] Apart from transamination, the catalyzed reactions include racemization, decarboxylation and retro-aldol cleavage.[7] In the *holo* enzyme, PLP is bound as a Schiff-base to a lysine residue in the active site, called the *internal aldimine* (E-PLP). The mechanism for PLP binding and formation of the internal aldimine in ornithine decarboxylase has recently been described by quantum chemical calculations, and it is suggested that a similar mechanism should be valid for most PLP-dependent enzymes.[8]

The detailed reaction mechanism of ωTAs has not been established. However, a mechanism similar to that of aspartate transaminase has been assumed in the literature.[4d,9,10] A common step in all PLP-dependent enzymes is the formation of a Schiff-base of PLP and an amino substrate, called the *external aldimine*, which replaces the lysine residue in the internal aldimine.[7] The steps involved in this transimination process have previously been studied computationally in the context of several other enzymes using models of various sizes.[11] The external aldimine has a lowered energy barrier for group abstraction from the nitrogen-binding carbon compared to the free amine substrate, and it is the point from which the reaction type is determined.[7] Proton abstraction may, for example, be performed by the lysine residue acting as a base. Scheme 1 shows a simplified half-transamination reaction mechanism, with (*S*)-1-phenylethylamine ((*S*)-1-PEA) as an amino donor, where the coenzyme-binding lysine subsequently acts as a base in the reaction. The reaction produces

Department of Organic Chemistry, Arrhenius Laboratory, Stockholm University, SE-106 91 Stockholm, Sweden. E-mail: fahmi.himo@su.se; Tel: +46 8 161094

†Electronic supplementary information (ESI) available: Additional figures of alternative transition states, table with absolute energies and energy corrections, and Cartesian coordinates of all optimized structures. See DOI: 10.1039/c5ob00690b

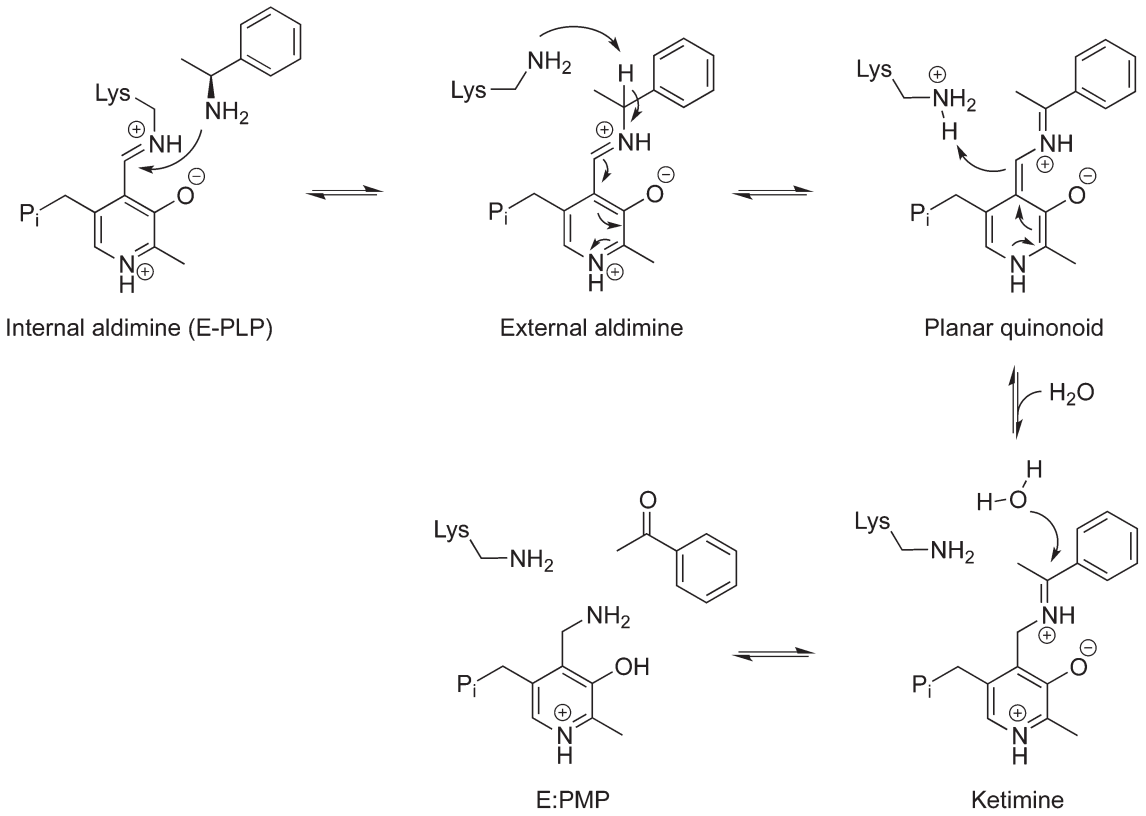

Scheme 1 Generally suggested half-transamination reaction where the (*S*)-1-phenylethylamine amino donor is converted to the corresponding ketone, acetophenone, while PLP is converted to PMP.

the corresponding ketone, acetophenone, while PLP is converted into pyridoxamine-5′-phosphate (PMP). A complete catalytic cycle includes the reverse reaction of another ketone, an amino acceptor, to regenerate E-PLP. By analogy to other transaminases, this scheme assumes that the reaction follows a bi-uni uni-bi ping-pong mechanism (not including the coenzyme PLP), which can be described as a ping-pong bi–bi mechanism by omitting the water substrate.[12] Scheme 2 shows the conversion of (*S*)-1-PEA, as an amino donor, to acetophenone while pyruvate, as an amino acceptor, is converted to L-alanine. In this case the equilibrium greatly favors the acetophenone and L-alanine products.[13]

ωTAs are a focal point in current biocatalysis research.[4,5] Discovery of homologues and construction of enzyme variants have yielded successful examples of how ωTAs may be engineered to cope with the demands of a specific synthesis.[5,6,14] In the present work, we focus on the reaction mechanism of ωTAs from *Chromobacterium violaceum* (Cv-ωTA). This enzyme has high homology to other known ωTAs and is biocatalytically useful.[15] Cv-ωTA has been crystallized,[16,17] and the crystal structure shows that the enzyme is a homodimer with two active sites located at the dimeric interface and consists of residues from both subunits.[17] The crystal structure further shows that the *holo* enzyme, in which PLP is bound to Lys288, undergoes a larger conformational change upon binding of PLP, where the phosphate group is bound in a so-called phosphate binding cup.[17]

Cv-ωTA can be applied for catalyzing the reaction in Scheme 2, which is useful for kinetic resolution purposes.[15] Due to the high stereospecificity of the enzyme toward 1-PEA,[18] when a racemate of this substrate is applied, (*S*)-1-PEA is consumed much faster than (*R*)-1-PEA, and the latter can thus be separated from the reaction mixture at a maximum theoretical yield of 50%. For stereoselective synthesis, the reversed reaction of Scheme 2, *i.e.* starting with L-alanine and acetophenone, gives (*S*)-1-PEA at a maximum theoretical yield of 100%, but requires equilibrium displacement since the products are disfavored.[3b,5a,c] As implied by Scheme 2, Cv-ωTA has the ability to accept hydrophobic amines and ketones as well as amino and keto acids as substrates.[15] It has been suggested that this feature may be explained by the presence of a flexible arginine residue that can flip to bind acidic substrates,[19] similarly to some other transaminases.[7a]

Herein, we use density functional theory (DFT) calculations to study the mechanism of the half-transamination of (*S*)-1-PEA to acetophenone in Cv-ωTA. A large model of the active site is devised and a full potential energy profile for the reaction is presented, along with geometries of intermediates and transition states. The adopted methodology has been used suc-

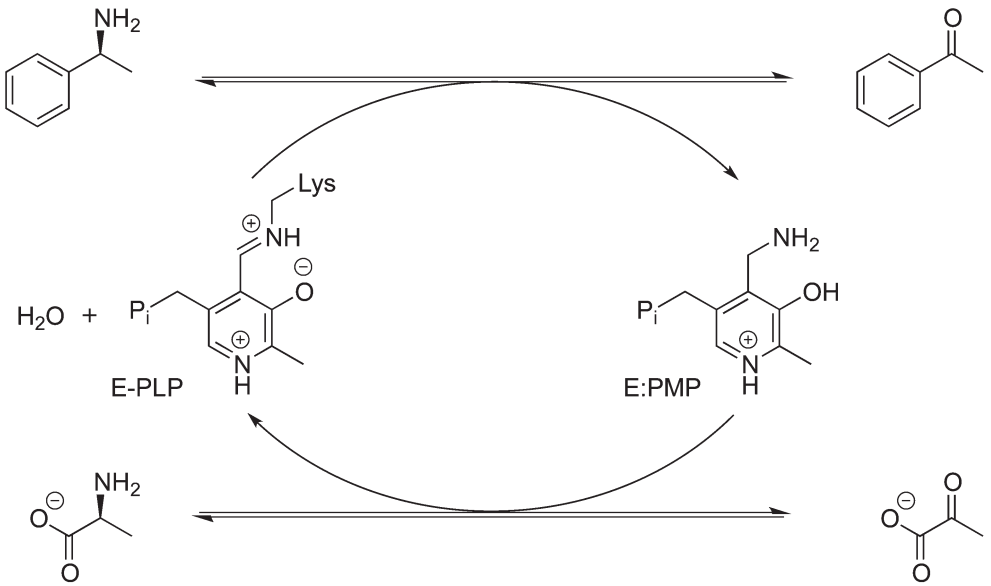

Scheme 2 Reaction scheme of a complete catalytic transamination cycle with (*S*)-1-PEA as an amino donor and pyruvate as an amino acceptor. PLP bound as a Schiff-base to a lysine residue, the internal aldimine, reacts with the amino donor which results in the formation of acetophenone with the consumption of a water molecule. The internal aldimine and the water molecule are then regenerated when the amino acceptor is converted to L-alanine.

cessfully to investigate a large number of enzyme reaction mechanisms.[20] Detailed knowledge of the reaction mechanism may further aid the development of rationally and semi-rationally designed enzyme variants.

II. Computational details

The calculations in this work were performed by DFT with the B3LYP functional,[21] using the Gaussian09 software package.[22] The 6-31G(d,p) basis set was used for the geometry optimizations followed by frequency calculations of the optimized geometries to obtain zero-point energy (ZPE) corrections. In the active site model, a number of atoms were kept fixed during the geometry optimizations (see below), which resulted in a number of small imaginary frequencies. These do not contribute significantly to the ZPE and can therefore be ignored. These small imaginary frequencies also result in the entropy calculations based on the rigid-rotor harmonic oscillator model being unreliable. However, the entropy is in general quite small in the chemical step of enzymatic reactions[23] and it is therefore a rather good approximation to neglect it in the cluster approach. The 6-31G(d,p) basis set was also used for single-point calculations of solvation effects for optimized geometries with the conductor-like polarizable continuum model (CPCM),[24] with $\varepsilon = 4$, in accordance with previous quantum chemical studies of enzyme mechanisms.[20] Based on the optimized geometries, more accurate energies were calculated by single-point calculations with the larger 6-311+G(2d,2p) basis set. Dispersion effects were added using the B3LYP-D2 method.[25]

III. Active site model

A model of the active site of Cv-ωTA, with residues from both subunits of the homodimeric enzyme, was constructed on the basis of the recent crystal structure of the *holo* enzyme (PDB 4A6T) with a resolution of 1.80 Å.[17] In addition to the substrates, (*S*)-1-PEA and water, the model consists of amino acid residues defining the binding pocket of the substrates (prime indicates a different subunit): Leu59, Trp60, Phe88′, Ile262, Tyr153, Phe22, Thr321′ and backbone elements between Gly230 and Ala231 (see Fig. 1). The Lys288 forming the Schiff base with the PLP cofactor is of course included, as well as Asp259 that forms a hydrogen bond with the nitrogen of the PLP. The residues were truncated at either the α- or β-carbons and hydrogen atoms were added manually. The phosphate group of PLP was removed, except for the bridging oxygen atom, which was saturated with a hydrogen atom and kept fixed. As mentioned above, it has been shown that phosphate binding in this enzyme induces a conformational change to yield the active form of the enzyme.[17] While structurally important, the phosphate group is assumed to not contribute significantly to the catalysis and was therefore omitted from the active site model.

The model consists of 197 atoms and has a total charge of 0. On the basis of initial preliminary geometry optimizations of the active site model, one or two centers on each residue were kept fixed in the geometry optimizations in order to preserve the overall structure of the active site and avoid large artificial movements as compared to the crystal structure. These centers are marked with asterisks in Fig. 1.

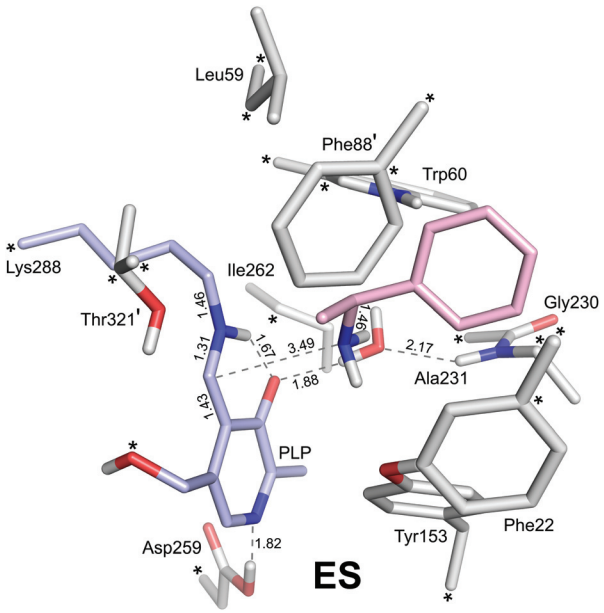

Fig. 1 Optimized structure of the Cv-ωTA active site model (**ES**) including the substrates (*S*)-1-PEA and water. Residues from one of the paired subunits are marked with primes. Atoms kept fixed at their crystallographic positions are indicated with asterisks. For clarity, non-polar hydrogen atoms have been omitted. Distances are given in Ångstrom (Å). The carbons of the substrate are colored in pink while the carbons of the Lys-PLP moiety are colored in light blue. Oxygens are in red and nitrogens in blue.

The amino group of the substrate was modeled in the neutral form. At the pH optimum of the enzyme (pH 8.3),[10] the majority of the (*S*)-1-PEA present in bulk solution should be protonated. However, we assume that the amino substrate loses a proton on entry into the active site in order for the reaction with the internal aldimine to occur.

Finally, in the general mechanism of Scheme 1, the pyridine nitrogen of PLP is schematically drawn to be in the protonated form. However, in the obtained mechanism (Scheme 3), the proton is located at the hydrogen bonding Asp259 residue throughout the reaction. The proton moves spontaneously from the nitrogen to the carboxyl group in the geometry optimization.

IV. Results and discussion

The half-transamination of (*S*)-1-PEA to acetophenone in Cv-ωTA was investigated by means of DFT calculations. The starting point of the investigation is the generally proposed mechanism shown in Scheme 1. The obtained detailed reaction mechanism is presented in Scheme 3. The optimized structures of transition states and intermediates are shown in Fig. 2–4, and the calculated overall potential energy graph is given in Fig. 5. The enzyme–substrate complex (**ES**), *i.e.* the optimized active site model containing the substrates (*S*)-1-PEA and water, is defined as the zero point (0 kcal mol^{-1}), to which all other energies are related.

A number of conformations and positions of the (*S*)-1-PEA and water substrates inside the active site model were tested, of which the one with lowest energy is shown in Fig. 1. In **ES**, the amino substrate is positioned with the phenyl group towards the opening of the active site and the amino group in a conformation suitable for nucleophilic attack on the internal aldimine, see Fig. 1. The substrate water molecule is hydrogen-bonded to the oxygen of PLP and the backbone nitrogen of Ala231. We note that the geometry optimization of **ES** resulted in small movements of some residues compared to their crystallographic positions, such as Leu59, Tyr153, Ala231 and Ile262, in order to accommodate the substrates in a more favorable manner.

In the first step of the proposed mechanism (Scheme 1), the substrate nitrogen performs a nucleophilic attack on the iminium carbon of the internal aldimine. The lowest barrier for this step (**TS1**) was found when the nucleophilic attack is accompanied by a concerted proton shuttling by the water molecule. That is, a proton from the substrate nitrogen is transferred to the oxygen of the water molecule, which simultaneously transfers another proton to the oxygen of PLP, see Fig. 2. The calculated barrier is 9.2 kcal mol^{-1} relative to **ES** and the resulting intermediate, in which both nitrogen atoms (of Lys288 and (*S*)-1-PEA) are bound to the PLP (**Int1**), is 4.3 kcal mol^{-1} higher than **ES**. In **TS1** the distance between the nitrogen of the substrate and the iminium carbon is 1.58 Å. To accomplish the proton shuttling, the hydrogen bond of the water molecule to the backbone amide of Ala231 is broken in **TS1** and then reformed in **Int1**. The diamine in **Int1** has a hydrogen bond between the proton on the oxygen of PLP and the nitrogen of Lys288, see Fig. 2.

A nucleophilic attack accompanied by a direct transfer of the proton from the nitrogen of the substrate to the oxygen of PLP, *i.e.* without the water molecule as a proton shuttle as in **TS1**, has a slightly higher barrier, calculated to be 10.6 kcal mol^{-1} relative to **ES** (*i.e.* 1.4 kcal mol^{-1} higher than **TS1**). In this case, the water molecule remains in the position of **ES** (see the ESI, Fig. S1† (**TS1′**)). A stepwise reaction, without concerted proton transfers, could not be found. Geometry optimization of the diamine with two protons on the substrate nitrogen, which would be the first intermediate in such a stepwise reaction, resulted in the dissociation of the substrate from the internal aldimine and the reformation of **ES**.

In the next step, the proton that was transferred to the oxygen of PLP is now transferred to the nitrogen of the lysine residue. The water molecule remains hydrogen-bonded to the oxygen of PLP and does not participate as a proton shuttle, in contrast to **TS1**, see Fig. 2. The energy for this transition state (**TS2**) is calculated to be 9.5 kcal mol^{-1} relative to **ES**, *i.e.* 5.2 kcal mol^{-1} higher than **Int1**. Utilizing the water molecule as a proton shuttle yielded a higher barrier, 4.0 kcal mol^{-1} above **TS2** (see the ESI, Fig. S1† (**TS2′**)). As shown in Fig. 2, **TS2** adopts a favorable six-membered transition state structure with N–H and H–O distances of 1.23 and 1.28 Å, respectively.

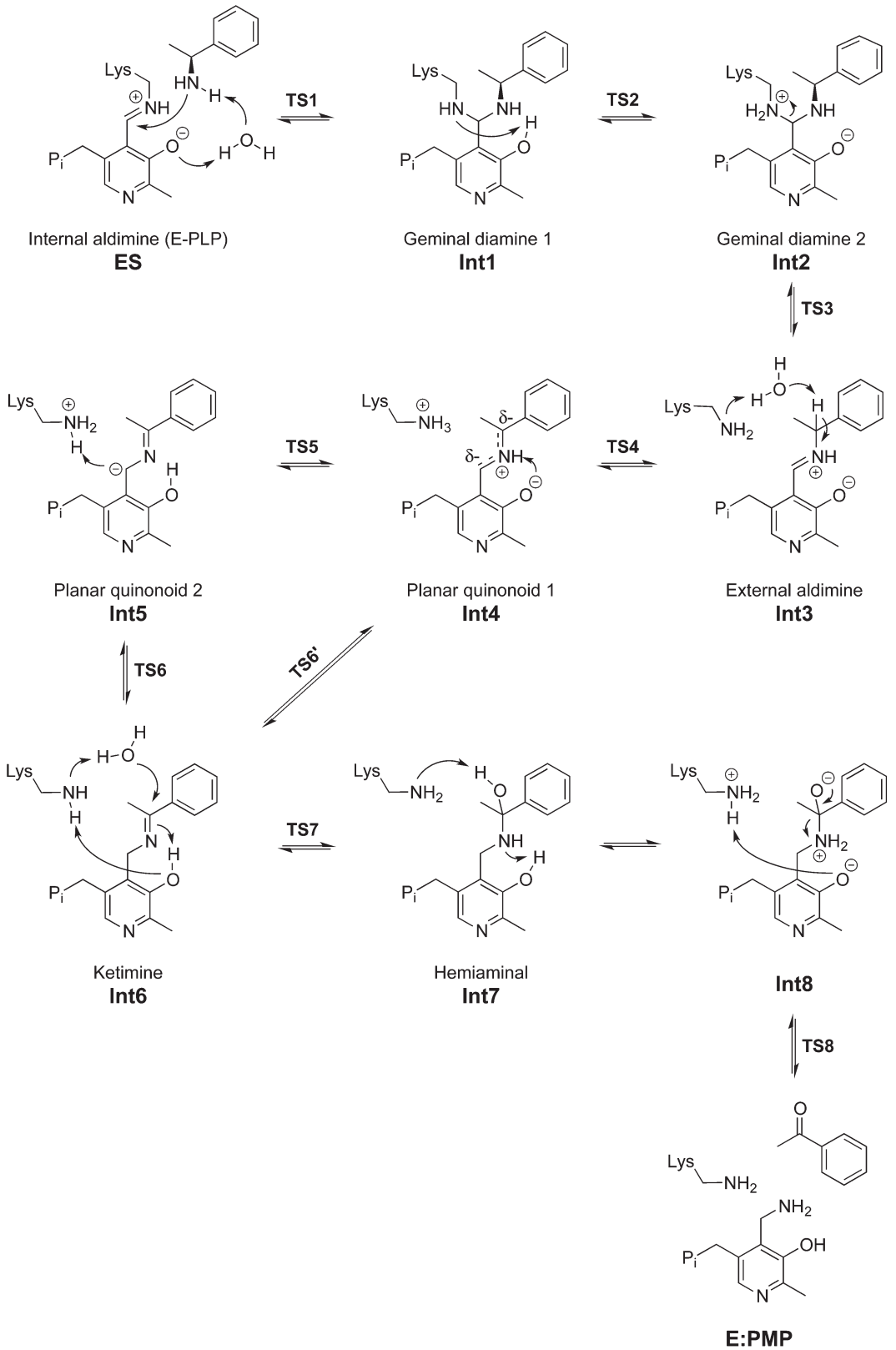

Scheme 3 Detailed reaction mechanism of Cv-ωTA-catalyzed half-transamination reaction of (*S*)-1-PEA to acetophenone.

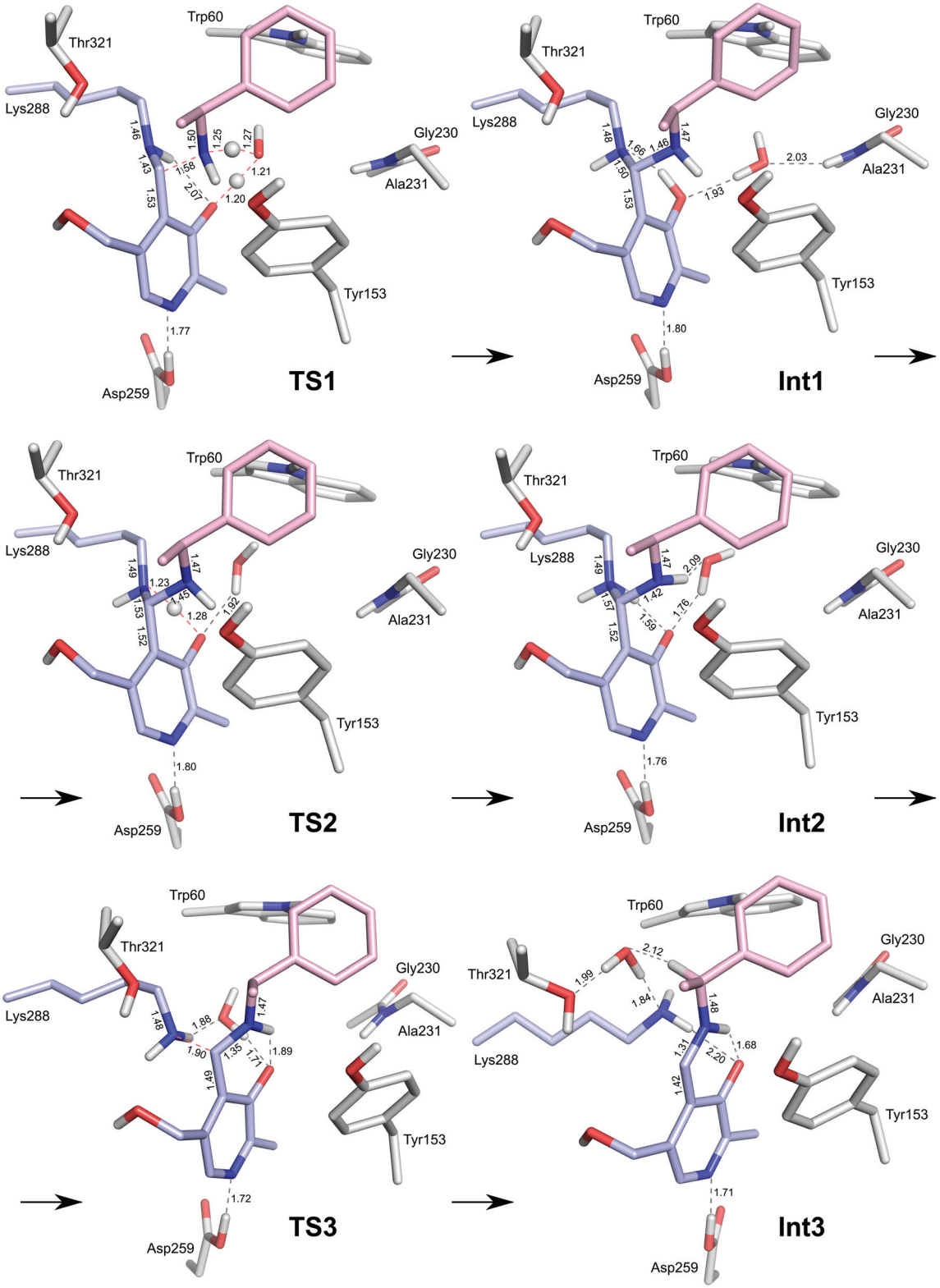

Fig. 2 Optimized structures of transition states and intermediates along the reaction pathway. For clarity, a number of elements and most non-polar hydrogen atoms have been omitted. The complete active site model is shown in Fig. 1. Note that the benzylic hydrogen of the substrate is also omitted in the figure up to **Int3**. For chemical structures, see Scheme 3.

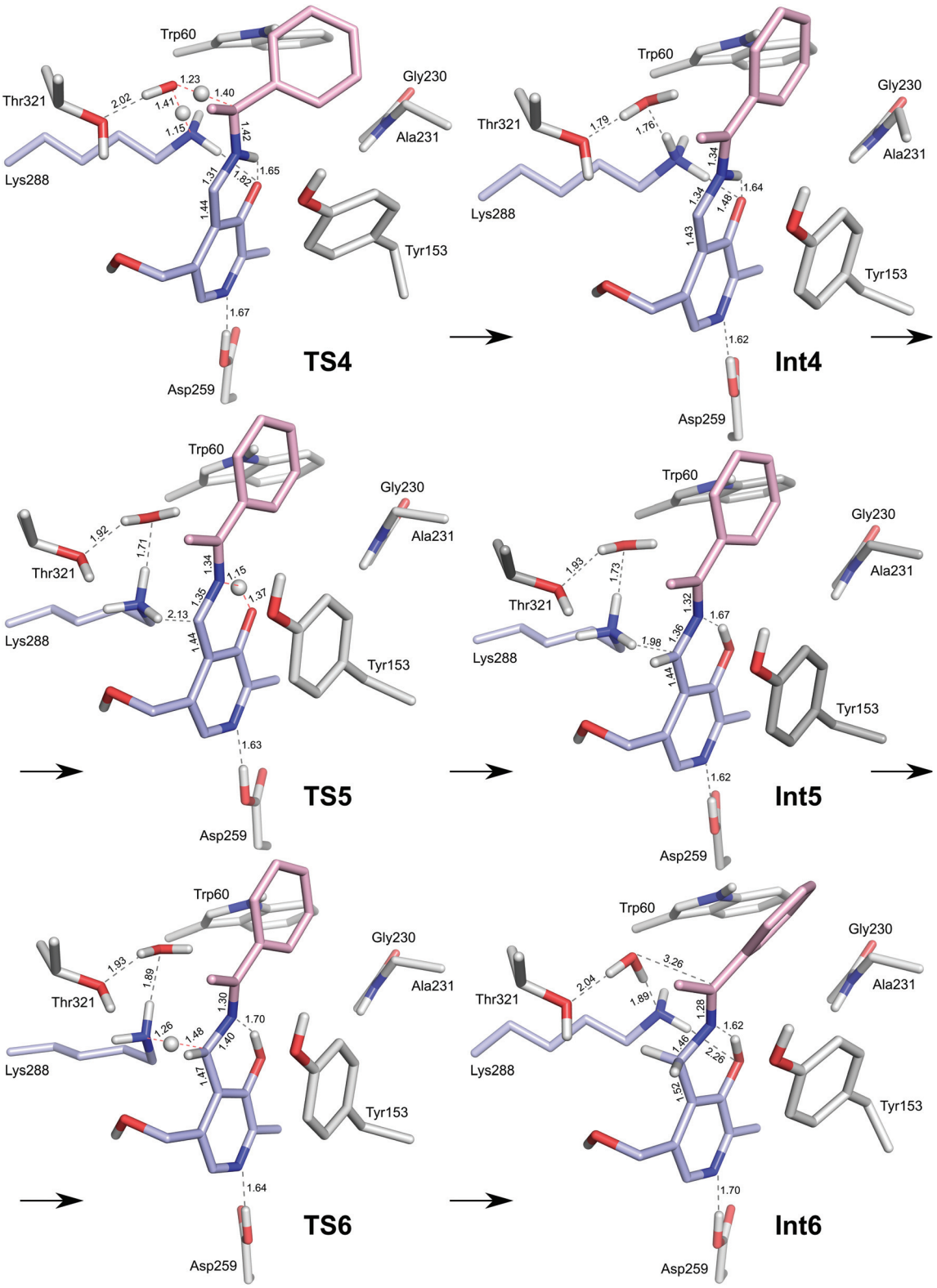

Fig. 3 Optimized structures of transition states and intermediates along the reaction pathway. For clarity, a number of elements and most non-polar hydrogen atoms have been omitted. The complete active site model is shown in Fig. 1 and the chemical structures are shown in Scheme 3. Note that the hydrogen on the carbon adjacent to the pyridine ring of the PLP is also omitted in the figure up to **Int5**.

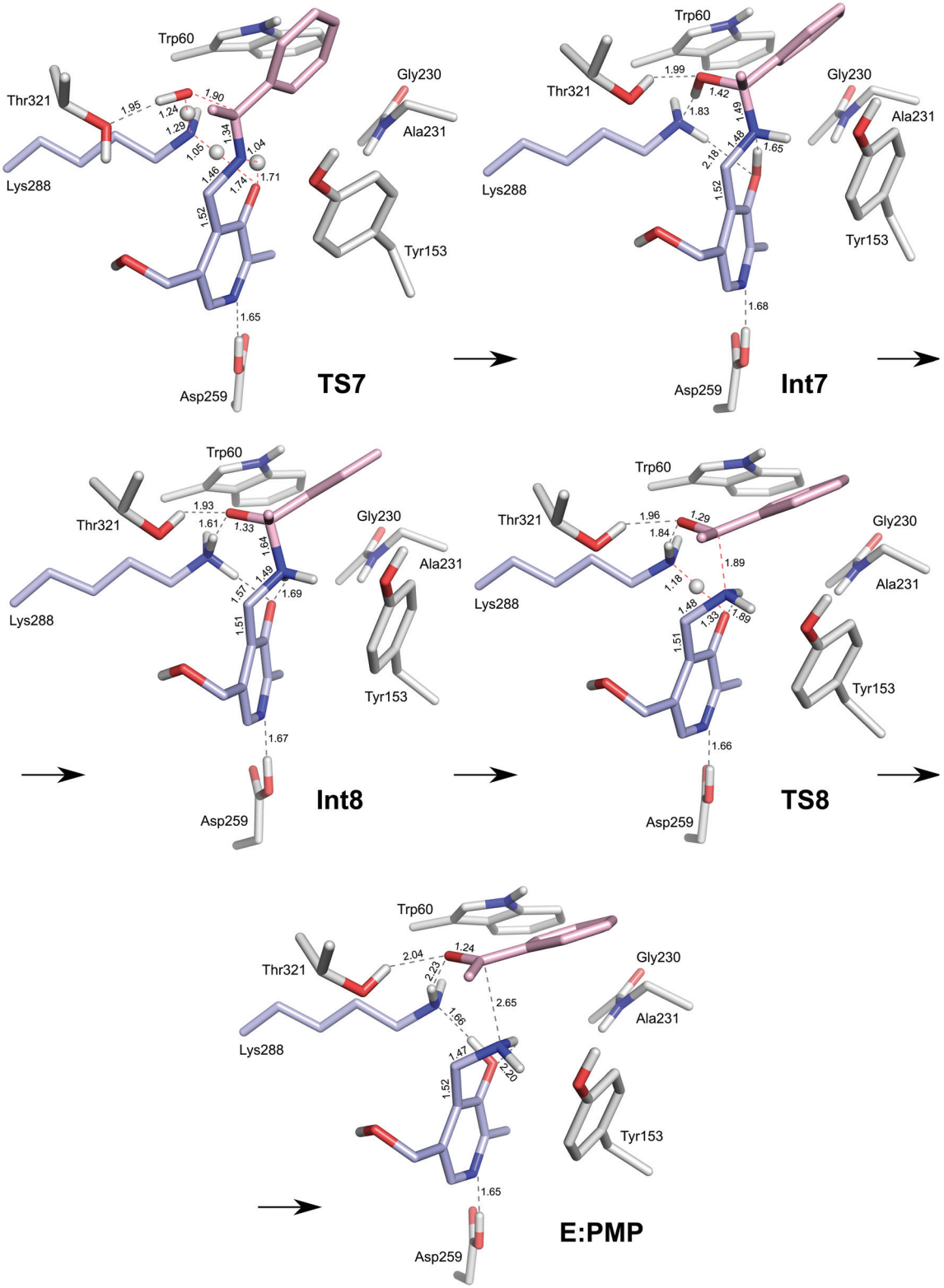

Fig. 4 Optimized structures of transition states and intermediates along the reaction pathway. For clarity, a number of elements and non-polar hydrogen atoms have been omitted. The complete active site model is shown in Fig. 1 and the chemical structures are shown in Scheme 3.

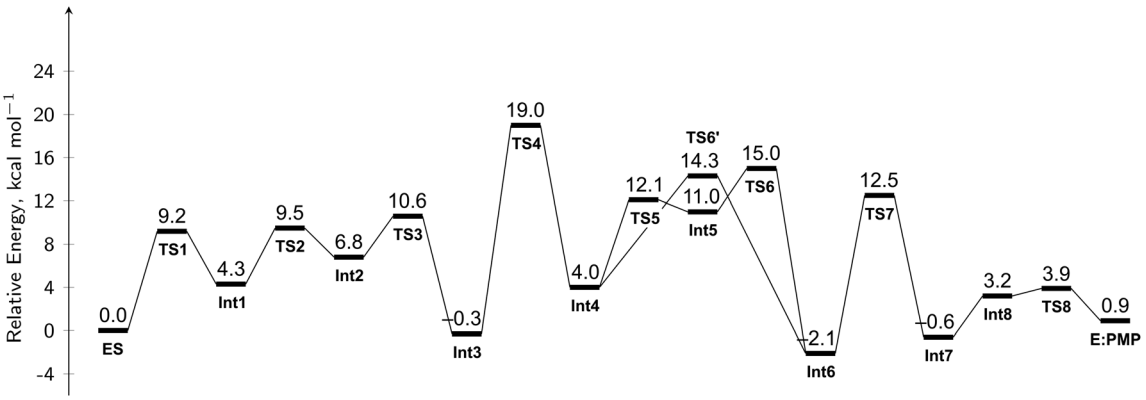

Fig. 5 Calculated energy profile for the half-transamination reaction of (*S*)-1-PEA to acetophenone in Cv-ωTA.

The resulting intermediate (**Int2**) has an energy of 6.8 kcal mol^{-1} relative to **ES**, *i.e.* 2.5 kcal mol^{-1} higher than **Int1**. In **Int2**, two protons are bound to the nitrogen of Lys288 without the cleavage of the bond to the carbon of PLP, see Fig. 2. Thus, in contrast to the concerted **TS1**, the analogous reaction of the lysine residue is stepwise.

In the following step, the bond between the nitrogen of Lys288 and PLP is broken. The transition state (**TS3**) has a calculated barrier of 10.6 kcal mol^{-1} relative to **ES**, or 3.8 kcal mol^{-1} from **Int2**. The resulting intermediate (**Int3**) is the external aldimine, which lies at −0.3 kcal mol^{-1} compared to **ES**. In **TS3**, the breaking C–N bond distance is 1.90 Å, with the water molecule hydrogen-bonded to the oxygen of PLP and the nitrogen of Lys288, see Fig. 2. At **Int3**, however, it was found that the water molecule moved to form a hydrogen bonding network with Thr321 and Lys288. Lys288 is also hydrogen-bonded to the oxygen of PLP, see Fig. 2.

Here, it should be pointed out that the steps described above, *i.e.* the transformation of the internal aldimine to the external aldimine, are consistent with previous computational work on other PLP-dependent enzymes where quite similar mechanistic paths were found, *i.e.* through geminal diamine intermediates.[11] The obtained energies are, however, quite different due to the different active site models used and also the different computational protocols adopted.

Next follows the proton abstraction from the external aldimine (see Scheme 1). The hydrogen-bonding network in **Int3** is suitable for proton shuttling through the water molecule, *i.e.* Lys288 abstracts a proton from the water, which simultaneously deprotonates the external aldimine, see the optimized transition state (**TS4**) structure in Fig. 3. As expected, the abstracted proton adopts a perpendicular configuration relative to the PLP–substrate plane.[7] The barrier for this step is calculated to be 19.3 kcal mol^{-1} relative to the external aldimine (**Int3**). The resulting intermediate **Int4**, the planar quinonoid, has an energy of 4.0 kcal mol^{-1} relative to **ES**. The bond distances of the iminium nitrogen to the carbon of the substrate and to the carbon of PLP are in **Int4** essentially equal, 1.34 Å, see Fig. 3. These can be interpreted as partial double bonds, as drawn in Scheme 3.

An alternative way to affect the proton abstraction from the external aldimine is the direct action of Lys288 as a base, *i.e.* without the water molecule as a proton shuttle. Following a small conformational change, Lys288 can be positioned in a favorable conformation for this transformation by hydrogen bonding to Thr321, while the water molecule in this case is hydrogen-bonded to the oxygen of PLP and to the backbone nitrogen of Ala231, as in **ES**. The barrier for this direct proton abstraction was calculated to be only 0.5 kcal mol^{-1} higher than **TS4** (see the optimized transition state structure in the ESI, Fig. S1† (**TS4′**)). The proton abstraction can thus take place with or without the assistance of the water molecule and the current calculations cannot distinguish between these two options.

In the next step, a proton from the protonated quinonoid nitrogen is transferred to the anionic oxygen of PLP. The transition state (**TS5**) has an energy of 12.1 kcal mol^{-1} relative to **ES**, *i.e.* 8.1 kcal mol^{-1} from **Int4**, and the resulting intermediate (**Int5**), which is also a quinonoid, is 7.0 kcal mol^{-1} above **Int4**. The proton transfer distances in **TS5** are calculated to be 1.15 Å for N–H and 1.37 Å for H–O. The water molecule remains hydrogen-bonded to Thr321 and Lys288, whereas Lys288 no longer forms a hydrogen bond with the oxygen of PLP but instead is well positioned for the next transition state, *i.e.* the formation of the ketimine, see Fig. 3. The C–N bonds at the imine nitrogen in **Int5** are no longer equal, as the bond length to the carbon adjacent to the pyridine group of PLP now is 0.04 Å longer than the bond length to the carbon of the substrate, indicating a slightly higher anionic character of the former carbon atom and a slightly more double bond character to the substrate.

In the following step, the carbon adjacent to the pyridine abstracts a proton from the protonated nitrogen of the lysine residue. The proton transfer to this carbon is favorable by the increased anionic nature achieved in **Int5**. Relative to **Int5**, this transition state (**TS6**) is 4.0 kcal mol^{-1}, and the resulting inter-

mediate, the ketimine (**Int6**), is −13.1 kcal mol^{-1}, *i.e.* −2.1 kcal mol^{-1} relative to **ES**. The N–H and H–C distances at **TS6** are 1.26 Å and 1.48 Å, respectively, see Fig. 3. The water molecule remains hydrogen-bonded to Thr321 and Lys288.

Here, it should be pointed out that by placing the water molecule in a position similar to that in **ES**, *i.e.* hydrogen-bonded to the oxygen of PLP and to the backbone nitrogen of Ala231, we could find a transition state (**TS6′**) that has 0.7 kcal mol^{-1} lower energy compared to **TS6** (see the ESI, Fig. S1†). In this case, it is found that this proton transfer from Lys288 to the carbon of PLP occurs concertedly with the proton transfer taking place in **TS5**, *i.e.* from the protonated quinonoid nitrogen to the anionic oxygen of PLP. Also in this case, it is not possible to distinguish between the two possibilities on the basis of the current calculations, and both options are therefore indicated in Scheme 3 and Fig. 5.

The next step is a nucleophilic attack by the water molecule on the imine carbon of the substrate. The reaction step is assisted by proton abstraction from the water molecule by Lys288, and positioning of the water molecule by hydrogen bonding to Thr321. In the optimized transition state (**TS7**) the forming O–C bond is perpendicular to the PLP–substrate plane, similarly to **TS4**, with a bond distance of 1.90 Å. The nucleophilic attack is accompanied by concerted proton transfers. An early proton transfer from the oxygen of PLP to the imine nitrogen is in **TS7** manifested by an N–H distance of 1.04 Å, and a late proton transfer from the nitrogen of the lysine residue to the oxygen of PLP by an H–O distance of 1.74 Å, see Fig. 4. **TS7** is 14.6 kcal mol^{-1} higher than **Int6**, *i.e.* 12.5 kcal mol^{-1} higher than **ES**. The resulting intermediate, the hemiaminal **Int7**, is −0.6 kcal mol^{-1} relative to **ES**.

Next, the oxygen of the hemiaminal is deprotonated by Lys288, with a concomitant proton transfer from the oxygen of PLP to the nitrogen of the hemiaminal, see Scheme 3. Relative to **Int7**, the optimized transition state for this transformation is calculated to be 2.7 kcal mol^{-1}, which is 1.1 kcal mol^{-1} lower than the resulting intermediate (**Int8**). This is of course an artifact of the adopted methodology, where geometry optimizations are performed in the gas phase with a medium-sized basis set, and the large basis set, solvation and dispersion effects are added as single-point energies. Therefore, the energy of **Int8**, at +3.8 kcal mol^{-1} relative to **Int7**, can effectively be considered as the barrier for this step. In **Int8**, the deprotonated oxygen of the hemiaminal is hydrogen-bonded to Thr321 and Lys288. The latter is also hydrogen-bonded to the oxygen of PLP, see Fig. 4.

The final step in the obtained mechanism is the cleavage of the C–N bond of the hemiaminal, accompanied by a concerted proton transfer from Lys288 to the oxygen of the coenzyme, to form acetophenone and PMP (**E:PMP**). The transition state for this step (**TS8**) is calculated to be 4.5 kcal mol^{-1} higher than **Int7**. In **TS8**, the breaking C–N bond distance is calculated to be 1.89 Å and the oxygen of the formed ketone is hydrogen-bonded to Thr321 and Lys288 as in **Int8**, see Fig. 4. The **E:PMP** complex is calculated to be 1.5 kcal mol^{-1} higher than **Int7**, *i.e.* +0.9 kcal mol^{-1} relative to the starting **ES** complex.

Upon dissociation of the formed ketone (see Fig. 4), the active site is available for the second substrate, *e.g.* pyruvate, for subsequent reformation of enzyme–PLP and the completion of the catalytic cycle.

It is interesting to follow how the water molecule moves during the reaction. In **ES** it is hydrogen-bonded to the backbone nitrogen of Ala231 and the oxygen of PLP. The former hydrogen bond is broken in **Int2**. Then, the water molecule is repositioned to hydrogen-bond to Thr321 in **Int3**, where it may act as a proton shuttle in **TS4** and remain in that position in the following steps until it is consumed in **TS7**. However, it cannot be excluded that a second water molecule can enter the active site after **TS3** as space might become available as a result of the dissociation of Lys288 from the coenzyme. This would then make the repositioning of the water molecule at **Int3** (as described above) unnecessary. This possibility has not been considered explicitly in the present study, but it would not change the mechanistic conclusions drawn here.

The calculated overall energy diagram for the reaction is shown in Fig. 5. According to this, the rate-determining step is the proton abstraction from the external aldimine, with a calculated energy barrier of 19.3 kcal mol^{-1} (**Int3** to **TS4**), which corresponds to a k_{cat} on the order of 0.1 s^{-1}. k_{cat} has not been measured explicitly for this enzyme, but the calculated value is reasonable considering that k_{cat}/K_M has been measured to be 0.68 s^{-1} mM^{-1} at 37 °C.[26] Here, it is interesting to note that the calculated barrier is quite similar to the barrier obtained by quantum chemical calculations of aspartate transaminase.[27] However, due to the different nature of the substrate, the proton transfer to the PLP carbon in the planar quinonoid (corresponding to **TS6** or **TS6′**) in that case has a higher energy than the proton abstraction from the substrate (corresponding to **TS4**).

The lowest energy point of the reaction is the ketimine, **Int6**, at −2.1 kcal mol^{-1} relative to **ES**. The reverse reaction has thus a calculated barrier of 21.1 kcal mol^{-1} (**Int6** to **TS4**), which is 1.8 kcal mol^{-1} higher than the forward reaction. Experimentally, when performed in aqueous medium, this half-transamination equilibrium reaction is greatly displaced by water, in favor of the ketone product.[10] The present results indicate that the ketone product is both kinetically and thermodynamically favored, since the backward reaction has a slightly higher barrier than the forward reaction. According to this, a putative mutation that can result in the stabilization of the external aldimine, but not the ketimine, may therefore alter the kinetic properties and be a more effective enzyme for stereoselective synthesis as it would lead to a faster formation of (*S*)-1-PEA than a reformation of acetophenone.

V. Conclusions

In this study, DFT calculations were used to study the detailed mechanism of the half-transamination reaction of (*S*)-1-PEA to acetophenone in Cv-ωTA. On the basis of the available crystal structure, a large model of the active site was constructed and

all intermediates and transition states were optimized. These are shown in Fig. 1–4 and the resulting energy profile for the reaction is presented in Fig. 5.

In the initial steps of the mechanism (Scheme 3), the calculations confirm that the amino substrate forms the external aldimine (**Int3**) with the PLP coenzyme through geminal diamine intermediates, in line with other studies. The model suggests that this external aldimine is then deprotonated by the active site lysine residue Lys288 in the rate-determining step (**TS4**) to form a planar quinonoid intermediate (**Int4**). It is followed by the formation of a ketimine (**Int6**), to which water is added to produce a hemiaminal intermediate (**Int7**). In the final step, deprotonation of the hemiaminal by lysine yields the product ketone and **E:PMP**.

This reaction mechanism and the associated energy profile are consistent with the available experimental data and the current calculations indicate thus that ω-transaminases might follow the same general mechanism as other transaminases.

We believe that the results presented here will be very valuable for guiding the experimental work to further improve the biocatalytic applicability of this important class of enzymes. We are currently using similar calculations to investigate other aspects of the ω-transaminase chemistry.

Acknowledgements

We acknowledge financial support from the Swedish Research Council, the Göran Gustafsson Foundation and the Knut and Alice Wallenberg Foundation. Computer time was generously granted by the Swedish National Infrastructure for Computing.

References

1 *Transaminases*, ed. P. Christen and D. E. Metzler, John Wiley and Sons, New York, 1985.
2 D. Voet, J. G. Voet and C. W. Pratt, *Fundamentals of Biochemistry: Life at the Molecular Level*, 2nd edn, Wiley, 2006.
3 (*a*) J. S. Shin and B. G. Kim, *Biotechnol. Bioeng.*, 1997, **55**, 348; (*b*) J. S. Shin and B. G. Kim, *Biotechnol. Bioeng.*, 1999, **65**, 206.
4 See for example the following reviews: (*a*) D. Koszelewski, K. Tauber, K. Faber and W. Kroutil, *Trends Biotechnol.*, 2010, **28**, 324; (*b*) P. Tufvesson, J. Lima-Ramos, J. S. Jensen, N. Al-Haque, W. Neto and J. M. Woodley, *Biotechnol. Bioeng.*, 2011, **108**, 1479; (*c*) M. S. Malik, E. S. Park and J. S. Shin, *Appl. Microbiol. Biotechnol.*, 2012, **94**, 1163; (*d*) P. Berglund, M. S. Humble and C. Branneby, in *Comprehensive Chirality*, ed. E. M. Carreira and H. Yamamoto, Elsevier, Amsterdam, 2012, pp. 390–401; (*e*) G. W. Huisman and S. J. Collier, *Curr. Opin. Chem. Biol.*, 2013, **17**, 284; (*f*) H. Kohls, F. Steffen-Munsberg and M. Höhne, *Curr. Opin. Chem. Biol.*, 2014, **19**, 180; (*g*) F. Steffen-Munsberg, C. Vickers, H. Kohls, H. Land, H. Mallin, A. Nobili, L. Skalden, T. van den Bergh, H.-J. Joosten, P. Berglund, M. Höhne and U. T. Bornscheuer, *Biotechnol. Adv.*, 2015, **33**, 566.
5 See for example: (*a*) M. Höhne, S. Kuhl, K. Robins and U. T. Bornscheuer, *ChemBioChem*, 2008, **9**, 363; (*b*) B. K. Cho, H. Y. Park, J. H. Seo, J. Kim, T. J. Kang, B. S. Lee and B. G. Kim, *Biotechnol. Bioeng.*, 2008, **99**, 275; (*c*) D. Koszelewski, I. Lavandera, D. Clay, G. M. Guebitz, D. Rozzell and W. Kroutil, *Angew. Chem., Int. Ed.*, 2008, **47**, 9337; (*d*) M. D. Truppo, N. J. Turner and J. D. Rozzell, *Chem. Commun.*, 2009, 2127; (*e*) M. D. Truppo, J. D. Rozzell, J. C. Moore and N. J. Turner, *Org. Biomol. Chem.*, 2009, **7**, 395; (*f*) U. Schell, R. Wohlgemuth and J. M. Ward, *J. Mol. Catal. B: Enzym.*, 2009, **59**, 279; (*g*) M. D. Truppo, J. D. Rozzell and N. J. Turner, *Org. Process Res. Dev.*, 2010, **14**, 234; (*h*) D. Koszelewski, M. Göritzer, D. Clay, B. Seisser and W. Kroutil, *ChemCatChem*, 2010, **2**, 73; (*i*) K. E. Cassimjee, C. Branneby, V. Abedi, A. Wells and P. Berglund, *Chem. Commun.*, 2010, **46**, 5569; (*j*) J. H. Seo, D. Kyung, K. Joo, J. Lee and B. G. Kim, *Biotechnol. Bioeng.*, 2011, **108**, 253.
6 C. K. Savile, J. M. Janey, E. C. Mundorff, J. C. Moore, S. Tam, W. R. Jarvis, J. C. Colbeck, A. Krebber, F. J. Fleitz, J. Brands, P. N. Devine, G. W. Huisman and G. J. Hughes, *Science*, 2010, **329**, 305.
7 (*a*) A. C. Eliot and J. F. Kirsch, *Annu. Rev. Biochem.*, 2004, **73**, 383; (*b*) M. D. Toney, *Arch. Biochem. Biophys.*, 2005, **433**, 279; (*c*) M. D. Toney, *Biochim. Biophys. Acta*, 2011, **1814**, 1407.
8 E. F. Oliveira, N. M. Cerqueira, P. A. Fernandes and M. J. Ramos, *J. Am. Chem. Soc.*, 2011, **133**, 15496.
9 M. Svedendahl, C. Branneby, L. Lindberg and P. Berglund, *ChemCatChem*, 2010, **2**, 976.
10 K. E. Cassimjee, M. S. Humble, V. Miceli, C. G. Colomina and P. Berglund, *ACS Catal.*, 2011, **1**, 1051.
11 (*a*) A. Salva, J. Donoso, J. Frau and F. Muñoz, *Int. J. Quantum Chem.*, 2002, **89**, 48; (*b*) A. Salva, J. Donoso, J. Frau and F. Muñoz, *J. Phys. Chem. A*, 2004, **108**, 11709; (*c*) Z. Zhao and H. Y. Liu, *J. Phys. Chem. B*, 2008, **112**, 13091; (*d*) N. M. F. S. A. Cerqueira, P. A. Fernandes and M. J. Ramos, *J. Chem. Theor. Comput.*, 2011, **7**, 1356; (*e*) M. Shoji, K. Hanaoka, Y. Ujiie, W. Tanaka, D. Kondo, H. Umeda, Y. Kamoshida, M. Kayanuma, K. Kamiya, K. Shiraishi, Y. Machida, T. Murakawa and H. Hayashi, *J. Am. Chem. Soc.*, 2014, **136**, 4525; (*f*) H.-P.-T. Ngo, N. M. F. S. A. Cerqueira, J.-K. Kim, M.-K. Hong, P. A. Fernandes, M. J. Ramos and L.-W. Kang, *Acta Crystallogr., Sect. D: Biol. Crystallogr.*, 2014, **70**, 596.
12 R. B. Silverman, *The Organic Chemistry of Enzyme-Catalyzed Reactions*, Academic Press, Elsevier Science, 2000.
13 J. S. Shin and B. G. Kim, *Biotechnol. Bioeng.*, 1998, **60**, 534.
14 See for example: (*a*) S. Pannuri, S. Kamat and A. R. M. Garcia, *World Pat*, WO2006/063336A2, Cambrex North Brunswick Inc., 2006; (*b*) J. S. Shin, B. G. Kim, A. Liese and C. Wandrey, *Biotechnol. Bioeng.*, 2001, **73**, 179; (*c*) J. S. Shin and B. G. Kim, *J. Org. Chem.*, 2002, **67**, 2848; (*d*) B. Y. Hwang and B. G. Kim, *Enzyme Microb. Technol.*,

2004, **34**, 429; (*e*) H. Yun, B. K. Cho and B. G. Kim, *Biotechnol. Bioeng.*, 2004, **87**, 772; (*f*) H. Yun, B. Y. Hwang, J. H. Lee and B. G. Kim, *Appl. Environ. Microbiol.*, 2005, **71**, 4220; (*g*) A. R. Martin, D. Shonnard, S. Pannuri and S. Kamat, *Appl. Microbiol. Biotechnol.*, 2007, **76**, 843; (*h*) B. Y. Hwang, S. H. Ko, H. Y. Park, J. H. Seo, B. S. Lee and B. G. Kim, *J. Microbiol. Biotechnol.*, 2008, **18**, 48; (*i*) D. Koszelewski, I. Lavandera, D. Clay, D. Rozzell and W. Kroutil, *Adv. Synth. Catal.*, 2008, **350**, 2761; (*j*) D. Koszelewski, D. Clay, D. Rozzell and W. Kroutil, *Eur. J. Org. Chem.*, 2009, 2289; (*k*) D. Koszelewski, D. Pressnitz, D. Clay and W. Kroutil, *Org. Lett.*, 2009, **11**, 4810; (*l*) M. Höhne, S. Schätzle, H. Jochens, K. Robins and U. T. Bornscheuer, *Nat. Chem. Biol.*, 2010, **6**, 807; (*m*) J. Ward and R. Wohlgemuth, *Curr. Org. Chem.*, 2010, **14**, 1914.

15 U. Kaulmann, K. Smithies, M. E. B. Smith, H. C. Hailes and J. M. Ward, *Enzyme Microb. Technol.*, 2007, **41**, 628.

16 C. Sayer, M. N. Isupov and J. A. Littlechild, *Acta Crystallogr., Sect. F: Struct. Biol. Cryst. Commun.*, 2007, **63**, 117.

17 M. S. Humble, K. E. Cassimjee, M. Håkansson, Y. R. Kimbung, B. Walse, V. Abedi, H.-J. Federsel, P. Berglund and D. T. Logan, *FEBS J.*, 2012, **279**, 779.

18 M. S. Humble, K. E. Cassimjee, V. Abedi, H.-J. Federsel and P. Berglund, *ChemCatChem*, 2012, **4**, 1167.

19 F. Steffen-Munsberg, C. Vickers, A. Thontowi, S. Schätzle, T. Meinhardt, M. S. Humble, H. Land, P. Berglund, U. T. Bornscheuer and M. Höhne, *ChemCatChem*, 2013, **5**, 154.

20 For recent reviews, see: (*a*) P. E. M. Siegbahn and F. Himo, *J. Biol. Inorg. Chem.*, 2009, **14**, 643; (*b*) M. R. A. Blomberg and P. E. M. Siegbahn, *Chem. Rev.*, 2010, **110**, 7040; (*c*) K. H. Hopmann and F. Himo, Comprehensive Natural Products Chemistry II Chemistry and Biology, in *Enzymes and Enzymatic Mechanisms*, ed. L. N. Mander and H.-W. Liu, Elsevier, Oxford, vol. 8, 2010, pp. 719–747; (*d*) P. E. M. Siegbahn and F. Himo, *Wiley Interdiscip. Rev.: Comput. Mol. Sci.*, 2011, **1**, 323; (*e*) M. R. A. Blomberg, T. Borowski, F. Himo, R.-Z. Liao and P. E. M. Siegbahn, *Chem. Rev.*, 2014, **114**, 3601.

21 (*a*) A. D. Becke, *J. Chem. Phys.*, 1993, **98**, 5648; (*b*) C. Lee, W. Yang and R. G. Parr, *Phys. Rev. B: Condens. Matter*, 1988, **37**, 785.

22 M. J. Frisch, G. W. Trucks, H. B. Schlegel, G. E. Scuseria, M. A. Robb, J. R. Cheeseman, G. Scalmani, V. Barone, B. Mennucci, G. A. Petersson, H. Nakatsuji, M. Caricato, X. Li, H. P. Hratchian, A. F. Izmaylov, J. Bloino, G. Zheng, J. L. Sonnenberg, M. Hada, M. Ehara, K. Toyota, R. Fukuda, J. Hasegawa, M. Ishida, T. Nakajima, Y. Honda, O. Kitao, H. Nakai, T. Vreven, J. J. A. Montgomery, J. E. Peralta, F. Ogliaro, M. Bearpark, J. J. Heyd, E. Brothers, K. N. Kudin, V. N. Staroverov, R. Kobayashi, J. Normand, K. Raghavachari, A. Rendell, J. C. Burant, S. S. Iyengar, J. Tomasi, M. Cossi, N. Rega, J. M. Millam, M. Klene, J. E. Knox, J. B. Cross, V. Bakken, C. Adamo, J. Jaramillo, R. Gomperts, R. E. Stratmann, O. Yazyev, A. J. Austin, R. Cammi, C. Pomelli, J. W. Ochterski, R. L. Martin, K. Morokuma, V. G. Zakrzewski, G. A. Voth, P. Salvador, J. J. Dannenberg, S. Dapprich, A. D. Daniels, O. Farkas, J. B. Foresman, J. V. Ortiz, J. Cioslowski and D. J. Fox, *Gaussian09 Revision A.02*, Gaussian, Inc., Wallingford CT, USA, 2009.

23 (*a*) P. Hu and Y. Zhang, *J. Am. Chem. Soc.*, 2006, **128**, 1272; (*b*) H. M. Senn, S. Thiel and W. Thiel, *J. Chem. Theor. Comput.*, 2005, **1**, 494; (*c*) H. M. Senn, J. Kästner, J. Breidung and W. Thiel, *Can. J. Chem.*, 2009, **87**, 1332.

24 (*a*) V. Barone and M. Cossi, *J. Phys. Chem. A*, 1998, **102**, 1995; (*b*) M. Cossi, N. Rega, G. Scalmani and V. Barone, *J. Comput. Chem.*, 2003, **24**, 669.

25 (*a*) S. Grimme, *J. Comput. Chem.*, 2006, **27**, 1787; (*b*) S. Grimme, J. Antony, S. Ehrlich and H. Krieg, *J. Chem. Phys.*, 2010, **132**, 154104.

26 K. E. Cassimjee, M. S. Humble, H. Land, V. Abedi and P. Berglund, *Org. Biomol. Chem.*, 2012, **10**, 5466.

27 R. Z. Liao, W. J. Ding, J. G. Yu, W. H. Fang and R. Z. Liu, *J. Comput. Chem.*, 2008, **29**, 1919.

